Nuclear relaxation during the formation of H_2 from spin-polarized hydrogen

Y. M. Xiao,* S. Buchman,* L. Pollack,† D. Kleppner, and T. J. Greytak
Department of Physics and Center for Materials Science and Engineering, Massachusetts Institute of Technology, Cambridge, Massachusetts 02139
(Received 17 July 1992; revised manuscript received 26 July 1993)

We report an NMR study of solid H_2 formed by the recombination of doubly polarized atomic hydrogen at a temperature of ~ 0.3 K. The molecules are formed in a highly excited ortho state with $M_I=-1$, thermalize through collisions with the ^{4}He-coated walls of the containment chamber, and form a solid. The solid is essentially pure ortho H_2 in the fcc phase, as expected. However, the nuclear polarization is close to zero, in contrast to the value of -1 if there was no relaxation, and $+0.034$ if the spin temperature was in equilibrium with the surface of the cell. Possible mechanisms for depolarization are discussed, though no plausible explanation for the loss has yet been found.

I. INTRODUCTION

The evolution of molecular hydrogen created by the recombination of spin-polarized hydrogen confined inside a cell coated by liquid helium has remained an enigma ever since spin-polarized hydrogen was first produced.[1] In the initial recombination event, two atoms form a molecule in a high-lying, weakly bound, vibrational state. More than 99% of the recombination energy is converted to internal energy of the molecule. At this stage, the protons are highly polarized. If the nuclear spins are unaffected as the molecule cascades down through the vibrational-rotational states to the ground state, the resulting solid will also be highly polarized. Such a polarized solid H_2 would be an attractive target for polarized proton-scattering experiments at high energies.[2] If these techniques were applicable to the other isotopes of hydrogen, polarized solid D_2 and T_2 might be used to enhance the efficiency of fusion reactions.[3,4]

In this paper, we report an NMR study of the evolution of the nuclear polarization following recombination.[5] We stabilize a gas of electron- and proton-polarized (doubly polarized) atomic hydrogen at low temperature (0.2 to 0.6 K) and high-magnetic field (6.7 T), and then trigger the recombination by flipping the electron spins with a microwave field. When atoms with opposite electron-spin orientation and the same nuclear-spin orientation recombine, nuclear-spin-polarized ortho molecules, ($I=1$, J odd) are produced. We monitor the polarization of the molecules using a pulsed-NMR spectrometer.

Our expectation was that the molecules would rapidly lose their vibrational and rotational energy through wall collisions, adsorb on the surface of superfluid helium, enter the liquid, and finally form a solid. Since the vibrational-rotational relaxation rate is large compared with the nuclear-spin relaxation rate, we expected that the nuclear-spin polarization would survive the deexcitation process. The experimental results presented in Sec. V indicate that this is not the case. Mechanisms for vibrational-rotational relaxation and nuclear-spin relaxation are discussed in Sec. VI.

II. BACKGROUND

Following the usual convention, the four hyperfine states of atomic hydrogen in a magnetic field are labeled **a**, **b**, **c**, **d**, in order of increasing energy. The state vectors are

$$|a\rangle=\cos\theta|-\tfrac{1}{2},\tfrac{1}{2}\rangle-\sin\theta|\tfrac{1}{2},-\tfrac{1}{2}\rangle\ , \tag{1}$$

$$|b\rangle=|-\tfrac{1}{2},-\tfrac{1}{2}\rangle\ , \tag{2}$$

$$|c\rangle=\cos\theta|\tfrac{1}{2},-\tfrac{1}{2}\rangle+\sin\theta|-\tfrac{1}{2},\tfrac{1}{2}\rangle\ , \tag{3}$$

$$|d\rangle=|\tfrac{1}{2},\tfrac{1}{2}\rangle\ , \tag{4}$$

where $|m_s,m_i\rangle$ denotes the projections of the electron and the proton spins along the magnetic field. The mixing angle θ is given by

$$\tan(2\theta)=\frac{a_H}{(\gamma_e+\gamma_p)B}=\frac{0.05061}{B}\ , \tag{5}$$

where a_H is the hydrogen hyperfine constant (1420 MHz), γ_e and γ_p are the electron and the proton gyromagnetic ratios (hertz/tesla), respectively, and B is the magnetic field in tesla. At a field of 6.7 T, $\theta=3.8\times10^{-3}$ and $(\sin\theta)^2=1.4\times10^{-5}$. Figure 1 shows that the energies of **a** and **b** decrease monotonically with B. Atoms in these states tend to be drawn into a region of increasing magnetic field and are referred to as "high-field seekers." Similarly, atoms in states **c** and **d** are low-field seekers. Electron polarization of atomic hydrogen occurs as the atoms impinge on a region of high-magnetic field, usually at the center of a superconducting magnet. Atoms in the **c** and **d** states are excluded from the high-field region; those in the **a** and **b** states enter, lose their excess energy through wall collisions, and become trapped. Axial confinement is provided by the magnetic-field gradient and radial confinement is provided by the walls of the experimental cell.

The electron-polarized gas of **a** and **b** atoms is not stable against recombination. The finite admixture of the "wrong" direction of electron spin in the **a** state due to

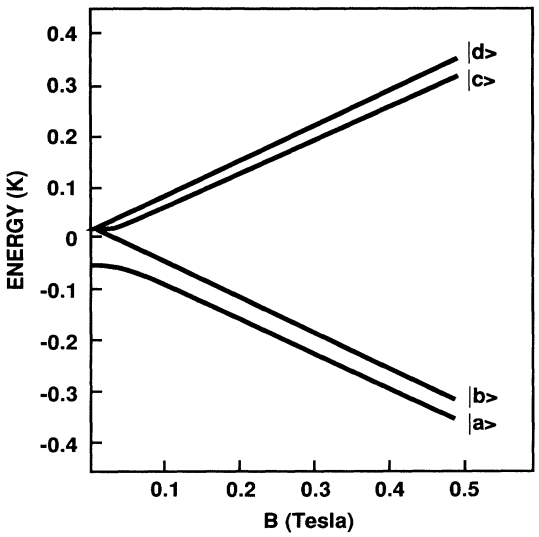

FIG. 1. The hyperfine structure of atomic hydrogen in modest magnetic fields. The experiments were carried out at a field of 6.7 T, where the *b*-*c* energy separation is 8.97 K (187 GHz) and the *a*-*b* separation is 48 mK (995 MHz).

hyperfine mixing allows the reactions $\mathbf{a}+\mathbf{b}\rightarrow$ ortho H_2, and $\mathbf{a}+\mathbf{a}\rightarrow$ para H_2. These reactions require a third body to satisfy conservation of energy and momentum. The third body could be another hydrogen atom but at the densities used in these experiments, the reaction takes place while the atoms are absorbed on the walls of the cell with the wall acting as the third body. Recombination is slowed but not eliminated by coating the walls of the cell with superfluid helium to minimize the van der Waals attraction between the atoms and the wall. The result of these reactions is to remove all of the **a** atoms while leaving a finite fraction of the **b** atoms. This gas of **b** atoms is nuclear as well as electron-spin polarized. It is long lived since two **b** atoms cannot recombine into a molecule.

There are two methods of obtaining polarized ortho H_2 from the doubly polarized atomic gas. The first is simply to wait. The doubly polarized gas is not absolutely stable. Each atom experiences a fluctuating magnetic field due to the electron moments of other passing hydrogen atoms. The fluctuating field causes the atom to relax from the **b** state to the **a** state. The newly created **a** atom quickly recombines with a **b** atom to produce an ortho molecule with the *z* component of total nuclear spin given by $M_I=-1$. Thus, one way to obtain nuclear polarized H_2 is to collect the decay products of doubly polarized atomic hydrogen.

Polarized molecules can be obtained on a much faster time scale by using microwave radiation to drive the $\mathbf{b}\rightarrow\mathbf{c}$ transition. The **c** atoms produced in this manner recombine quickly on the surface with the existing **b** atoms to produce ortho H_2 in the $M_I=-1$ state. There is a competing mechanism by which a **c** atom can disappear. It can undergo a spin-exchange collision, $\mathbf{c}+\mathbf{a}\leftrightarrow\mathbf{d}+\mathbf{b}$, with the subsequent production of a para H_2 as the **d** atom recombines with a **b** atom. Detailed balance applied to the spin-exchange process leads to a relation between the densities of the **c** and **d** atoms: $n_d/n_c=n_a/n_b$. Consequently, once atoms are driven to the upper states by the microwaves, one expects that $n_d \ll n_c$ and the production of para H_2 should be negligible. Both methods of producing polarized H_2, nuclear relaxation, and microwave transition, were used in the experiments reported here.

The excited molecule H_2^* formed in the recombination process,

$$H+H+M\rightarrow H_2^*+M\ , \tag{6}$$

will be in some vibration-rotation state (v,J). M is a third body whose participation is required by the need to conserve energy and momentum. The characteristic energy separation between vibration-rotation states near the dissociation limit is about 60 K. If the molecule was formed in a state above the dissociation limit, the energy deficit would have to be made up by the initial kinetic energy which can be no more than a few kelvin in these experiments. When a molecule is formed in a state below the dissociation limit, the excess energy is carried off by the third body and the translational motion of the molecule. The overlap integrals in the transition matrix elements decrease rapidly as the final kinetic energy increases. Quantum statistics require that ortho H_2 ($I=1$) must have odd J and para H_2 ($I=0$) must have even J. These general considerations suggest that at low temperatures, recombination can result in only a small number of initial molecular states. Theoretical studies of gas phase recombination in which the third body is either a He atom[6] or a H atom,[7] indicate that at $T<1$ K the ortho channel is dominated by the $v=14$, $J=3$ state and the para channel is dominated by the $v=14$, $J=2$ state. We are not aware of any theoretical study of recombination of H atoms physisorbed on superfluid helium surfaces. A calculation[8] for recombination of physisorbed H atoms on a Xe crystal surface at 4 and 10 K shows that the dominant ortho channel is $v=14$, $J=5$. Based on these considerations, the dominant ortho channel for recombination of physisorbed H atoms on superfluid helium surfaces is expected to be the $v=14$, $J=3$ state.

Of the 50 000 K binding energy of molecular hydrogen, less than 1% is transferred to translational kinetic energy during the formation of the weakly bound state. Where and how the remainder of the binding energy is released has important implications for the nuclear-spin polarization. Because the energy is stored predominantly as vibrational excitation, we shall refer to this process as vibrational relaxation.

Vibrational relaxation of molecules in the $v=1$ state has been studied extensively. In the gas phase, the cross section for relaxation $v=1\rightarrow 0$ decreases with temperature from 250 to about 100 K, then remains temperature independent to the lowest temperature studied so far, 40 K. This has been found experimentally[9] for H_2^* in H_2, and theoretically[10] for H_2^* in He. The two studies are in close agreement. The low-temperature cross section is $\sigma_{1,0}=3\times 10^{-23}$ cm^2, a value that is so small compared to

the geometrical cross section that the molecule can undergo a huge number of collisions without changing its vibrational state. The vibrational relaxation rate γ is described by

$$\gamma_{1,0}=\sigma_{1,0}nv_r \ , \tag{7}$$

where v_r is the mean relative velocity and n is the atomic density. Assuming the above value for the low-temperature cross section, the relaxation time for a density of $n=10^{16}$ cm^{-3} at a temperature of 0.3 K would be over 100 s.

In contrast to gas phase relaxation, molecules that are adsorbed on the surface or submerged in the liquid can relax rapidly. Studies by Delande and Gale[11] of vibrational relaxation in gaseous, liquid, and solid H_2 at temperatures down to 14 K indicate that the vibrational relaxation time varies linearly with the interparticle spacing. In liquid H_2 at 14 K, the relaxation time for the $v=1$ state is 12 μs. This suggest that molecules in the $v=1$ state will relax on a similar time scale when they are in close contact with liquid helium.

Laboratory observations of molecules in high-vibrational states have been realized only recently[12,13] and little is known about the relaxation rates. The high-vibrational states have relatively large geometrical cross sections and transitions between them have relatively small energy defects. It is reasonable to expect that the relaxation rates for molecules in high-vibrational states are much larger than those for the low-vibrational states in a similar environment. Thus, the vibrational relaxation time for high-vibrational states is expected to be shorter than 100 s when they are in the gas phase (assuming a gas density of 10^{16} cm^{-3} and temperature of 1K) and shorter than 10^{-5} s when they are in close contact with liquid helium.

Kurten and Ristig[14] have examined theoretically the interaction of atomic and molecular hydrogen with liquid helium. They report a value for the chemical potential μ for replacing a helium atom in the liquid with a hydrogen molecule of $\mu=-18$ K. The fact that μ is negative means that H_2 will enter liquid helium. In contrast, the chemical potential for atomic hydrogen in liquid helium is positive and the atoms either remain in the gas phase or are adsorbed on the surface. The interaction between a helium atom and a hydrogen molecule, an important factor in the chemical-potential calculation, is expected to depend on the vibration-rotation state (v,J). Based on the results of Kurten and Ristig, it is reasonable to expect that vibrational relaxation of molecules in the lower excited states will occur in the liquid. Where the vibrational relaxation of highly excited molecules occurs remains an open question.

In designing the experiment, we assumed that vibrational relaxation would occur predominantly on the surface or in the liquid. Vibrational relaxation is not expected to alter the nuclear spin. The nuclear spins are coupled to the rotational motion of the molecule, but the spin-rotation interaction is not expected to relax the nuclei in a strong applied field. Thus, it is plausible that the molecules could relax to their ground vibrational-rotational state without losing their nuclear polarization.

As the concentration of polarized ortho hydrogen increases on or in the liquid He, the molecules will condense to form a solid. The phase diagram for bulk solid ortho hydrogen[15] shows that the fcc phase is stable below about 3 K. In this phase the spins relax with a time constant T_1 given by[16]

$$T_1=AX^4T^{-1}e^{(B+0.24)/T} \ , \tag{8}$$

where X is the ortho concentration, $A=1.0(3)$ min and $B=0.4(1.8X-1.0)$ K. For pure ortho hydrogen at 0.3 K, one expects that $T_1=21(8)$ min. Above 3 K, the stable solid phase of ortho hydrogen is hcp. T_1 in this phase is of the order of milliseconds.[17] It is also possible that the conditions under which the H_2 molecules aggregate[18] lead to the formation of a nonequilibrium, low density, filamentary phase of solid hydrogen next to the wall. The value of T_1 in such a configuration would be difficult to predict. Eventually, in the solid phase ortho hydrogen ($I=1$) will convert to a para hydrogen ($I=0$) according to[15]

$$\frac{dX}{dt}=-kX^2 \ , \tag{9}$$

where $k=0.0190(5)$ h^{-1}.

Experiments described in the following sections indicate that the nuclear polarization is destroyed in a time comparable to or shorter than one second. This leaves the molecules in a state with $I=1$, but $\langle M_I \rangle=0$.

III. APPARATUS AND TECHNIQUES

Hydrogen atoms are formed from a gas of molecular hydrogen in a radio-frequency dissociator operated at 77 K. The unpolarized atoms pass through a tube lined with molecular hydrogen at about 10 K, traverse a short transition region and pass down a superfluid helium-lined vertical tube cooled by a dilution refrigerator. Electron polarization occurs when the atoms at a temperature of about 0.3 K encounter the 6.7 T field of a superconducting magnet. The flux of electron polarized atoms is about 8×10^{14} atoms s^{-1}. A detailed description of this part of the apparatus has been given elsewhere.[19]

A. Sample cell

Nuclear polarization of the gas occurs in the high-field region as a-state atoms recombine. It is desirable to exclude the para H_2 formed during this process from the region where the recombination of the doubly polarized gas is studied. In order to accomplish this, the cell is divided into two regions: a polarization chamber and an NMR chamber.

The cell is illustrated in Figs. 2 and 3. At the center of the cell is the NMR chamber, a cylindrical can of inside diameter 1.8 cm and inside length 2.0 cm. The NMR coil is wound on a sapphire cylinder which excludes atoms from a region along the axis of the chamber. The accessible volume of the NMR chamber is 3.7 cm^3 and it has a surface area of 25.5 cm^2. The NMR chamber is positioned inside a concentric cylindrical polarization chamber where the electron-polarized atoms acquire a

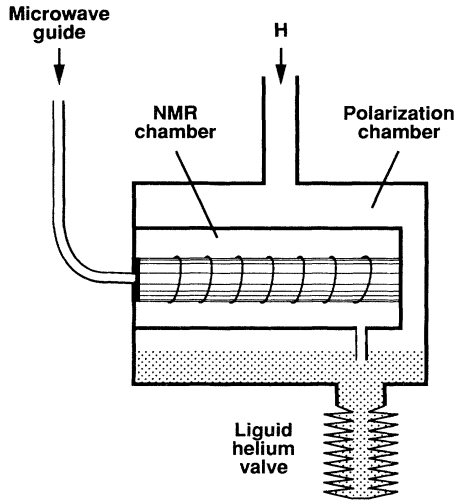

FIG. 2. Schematic diagram of the experimental cell.

nuclear polarization. The two chambers are linked by a liquid-helium valve. Electron-polarized atoms enter the housing through a tube from above. The polarization chamber consists of the space between the cylindrical housing 3.10 cm in diameter and 3.81 cm long, and the NMR chamber, plus the region of the filling tube which is located in the high field. The volume of the polarization chamber is 13.4 cm^3. A pressure transducer attached to the polarization chamber allows us to determine the gas density. The polarization of the atomic gas is derived from the evolution of the density as the atomic gas undergoes two-body decay.

The two chambers are connected by a 1 cm length of 0.11 cm diameter tube protruding from the bottom of the NMR chamber. The chambers can be isolated from each other by raising the level of liquid helium that is stored in a bellows under the cell. A coil is wound around the lower end of the bellows, in the high-gradient region of the magnet. Applying current to this coil expands the bellows and lowers the helium level in the cell. The time for the atomic hydrogen gas to fill the NMR chamber by molecular flow through the small tube is calculated to be 1.5 s.

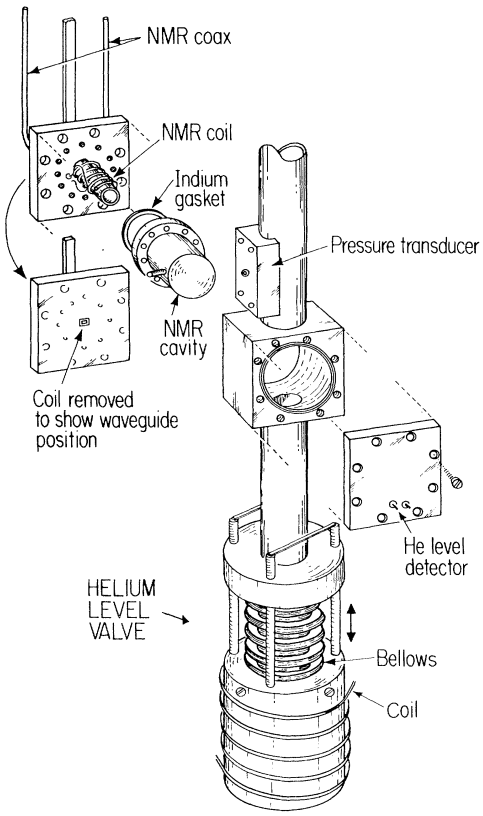

FIG. 3. Pictorial diagram of the experimental cell. In this figure the NMR cavity has been rotated 90° about its axis to show the inlet tube. The inlet tube normally points downward.

B. Electron-spin-resonance system

Figure 4 shows the microwave system. Microwaves are generated by a Varian klystron, model VC-738, which covers a frequency range from 182.9 to 188.3 GHz with an output power greater than 10 mW. An attenuator allows us to adjust the power level. Fundamental mode waveguides made of coin silver are used at the two ends of the transmission path where the waveguides must be bent for proper fitting. The center region of the transmission path, where low-thermal conductivity is important, consists of an over mode stainless steel waveguide with 0.25 mm thick walls which are silver coated (0.001 mm) on the inside. Transitions between the two different sized waveguides are made by copper horns. Thin Kapton (0.012 mm) films between the fundamental waveguides and the horns serve to keep the center section vacuum tight. The center section is thermally anchored to the 4 K bath, the cold plate, the still, the base plate, and the mixing chamber of the refrigerator. To reduce the

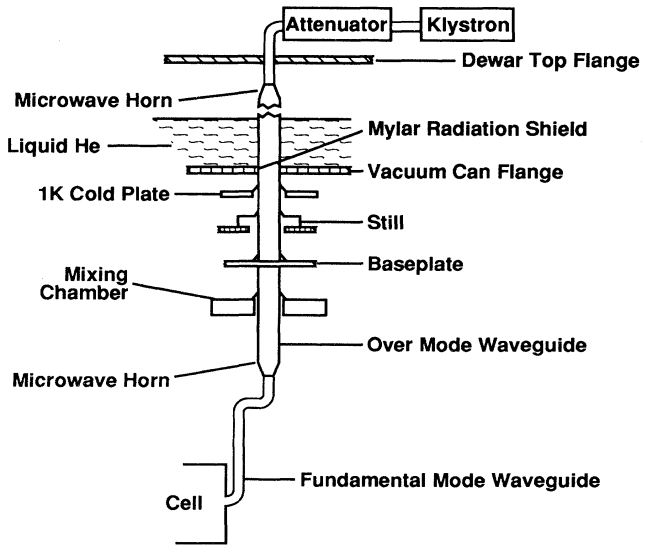

FIG. 4. Schematic diagram of the ESR system.

thermal radiation along the waveguide, a thin Mylar (0.08 mm) sheet is placed inside the waveguide near the vacuum can flange. With these arrangements, the power attenuation from the klystron to the mixing chamber is 13 dB (measured at room temperature). At a temperature of 0.3 K, the maximum power reaching the mixing chamber is 600 μW. This was determined by monitoring the load placed on the dilution refrigerator by the microwave radiation.

As shown in Fig. 2, the waveguide is sealed from the NMR chamber by a sapphire tube. This allows the microwaves to enter the cavity while preventing the escape of hydrogen atoms or molecules. The NMR chamber forms a nonresonant electron-spin-resonance (ESR) cavity. The resonance linewidth for the microwave transition is about 2 MHz and is dominated by the inhomogeneity of the magnetic field.

C. Nuclear-magnetic-resonance system

A block diagram of our pulsed-NMR spectrometer is shown in Fig. 5. By changing a few components the spectrometer can be tuned from 250 MHz to 1.5 GHz. The frequency stability is 10^{-9}, determined by the stability of the synthesizer. A word generator (programmable switch) enables a pulse sequence to be established with 10 ns resolution, but the response time of the spectrometer is limited to 5 μs by the 300 KHz bandwidth of the low-frequency amplifier. A digitizer with 8-bit resolution can sample data at rates as high as 32 MHz. The noise level

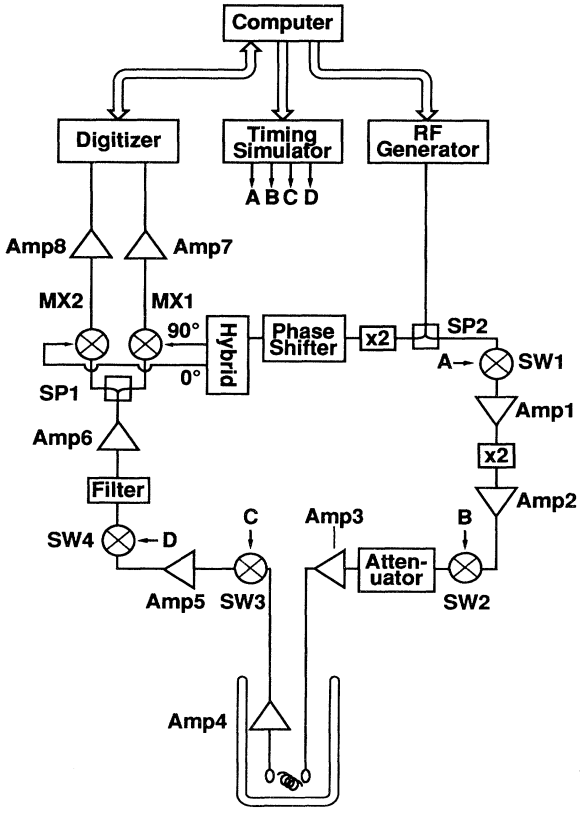

FIG. 5. Block diagram of the NMR spectrometer.

of the spectrometer is determined by the cooled amplifier which has a noise temperature less than 30 K.

The nuclear-spin polarization of ortho hydrogen is defined as

$$P_n=\frac{(N_0-N_{-1})+(N_1-N_0)}{N}\ , \tag{10}$$

where N is the number of ortho molecules and N_M is the number of molecules in the spin state M. The power radiated from ortho hydrogen, after a $\pi/2$ pulse, decreases in time according to

$$P_{\text{signal}}=\frac{\omega_I\mu_0 Q M_n^2}{4}\frac{\eta}{V_s}\exp\left[-\frac{2t}{T_2}\right]\ , \tag{11}$$

where $M_n=\gamma_p hNP_N$ is the nuclear magnetization, $\omega_I=2\pi\times 284$ MHz is the proton precession frequency in the 6.7 T field, η is the NMR cavity filling factor, V_s is the cell volume, and T_2 is the sample's transverse relaxation time. The NMR cavity has a quality factor $Q=300$. The receiving loop is nearly critically coupled, and the transmission loop is slightly undercoupled. We calibrated the spectrometer with a normal molecular hydrogen gas at 30 and 77 K, and found $\eta=0.1$. Substituting the known values into Eq. (11), we obtain

$$P_{\text{signal}}=10^{-42}(NP_N)^2\exp\left[-\frac{2t}{T_2}\right]W\ . \tag{12}$$

The spectrometer noise level, as mentioned earlier, is less than 300 K. For a 300 kHz bandwidth, the noise power is

$$P_{\text{noise}}<4kT_{\text{noise}}\delta f=5.0\times 10^{-16}\ \text{W}\ . \tag{13}$$

The transverse relaxation time constant T_2 is determined by the field inhomogeneity. For the calibration gas, $T_2=28.5$ μs; for the solid sample produced from the recombination, $T_2=3.5$ μs. The dead time, defined as the time lag between the excitation pulse and the first data point of the free-induction decay recorded, is typically less than 5 μs. We, therefore, could expect to detect a gas of 4×10^{13} fully polarized molecules and a solid of 10^{14} fully polarized molecules.

Despite having taken great care to exclude impurities from the NMR cavity, we found a background NMR signal equivalent to 2.3×10^{17} polarized protons. Most of this signal could be saturated. Typically, after scanning the cavity with 16 μW of power near the cavity-center frequency of 284 MHz for 20 s, the background signal is saturated to a level of less than 5×10^{15} polarized protons. The background signal recovers from saturation with a time constant of 30 h. The uncertainty associated with each saturation effect was at the level of 5×10^{14} polarized protons. This determines the limit of sensitivity of the experiment.

IV. PROCEDURE

Experiments were carried out at temperatures from 0.1 to 0.6 K, using walls coated with either pure ^{4}He or a ^{3}He–^{4}He solution. Both nuclear relaxation and mi-

crowave resonance were used to create the molecules. The creation of molecules at 0.3 K by microwave resonance, using ^{4}He as the surface coating, will be discussed in detail; results obtained under other experimental conditions will be mentioned briefly.

At the beginning of a run, the NMR chamber was closed by the liquid-helium value. There was no atomic hydrogen in the cell. The atomic source was turned on and allowed to run until the density and polarization of atoms in the cell reached a steady-state value. Typically, after 40 min a partially polarized gas of density of 3.2×10^{16} atoms cm^{-3} had accumulated in the polarization chamber. The source was then turned off and the atomic hydrogen gas was allowed to acquire nuclear polarization by selective recombination of the **a** and **b** states for an additional 20 min. During this period the density decreased to 1.6×10^{16} atoms cm^{-3} and the nuclear polarization reached approximately 96%.

While the atoms were developing nuclear polarization outside the NMR chamber, the residual protons within the NMR chamber that cause the background signal were driven into saturation. A cw signal was scanned around the proton resonance frequency 284 MHz for about 20 s. This was done twice. After the first saturation, the signals due to the recovering protons were recorded and stored for future use. The second saturation was performed just before the atoms were admitted into the NMR chamber.

After the gas had developed a high nuclear polarization and the background had been saturated, the liquid-helium valve was opened. The gas density dropped to 1.3×10^{16} atoms cm^{-3} due to expansion into the larger volume. Five seconds later, molecular recombination was initiated by driving the **b**$\rightarrow$**c** transition with a 60 μW microwave signal at the transition frequency of 187 GHz. After about 50 s all the atomic hydrogen in the cell, in both the polarization chamber and the NMR chamber, had recombined.

By design, the recombination took place only in the NMR chamber. We determined that the molecules remained in the NMR chamber after they recombined by using the following technique. Recombination was induced with the valve open and the subsequent NMR signal (proportional to the number of molecules in the NMR chamber) was measured. In a separate run, starting with the same atomic density, the valve was closed before recombination was induced and the NMR signal was again measured. The ratio of the two NMR signals was, to within about 20%, the ratio of the total volume to the NMR chamber volume. This result demonstrates that the time required for the molecules to condense on the walls of the NMR chamber was short compared to the time for effusion from the chamber. Consequently, an average molecule remained in the gas for a time less than the effusion time, 1.5 s.

The time evolution of the nuclear magnetization of the molecules was monitored by free-induction decay using a tipping angle of less than 10°. Each measurement consisted of a pattern of three decay signals, separated in frequency by 100 KHz. Measurements commenced 5 s after the microwave-induced recombination began and were repeated every 30 s for half an hour. The long-term behavior of the magnetization was monitored by repeating the pattern every 30 min for 65 h.

V. OBSERVATIONS

A. Studies of the nuclear polarization

Because the background proton NMR signal was large, the first data we present show the effect of saturating the background. The free-induction decays shown in Figs. 6(a) and 6(b) were taken about 10 s after the background was saturated for the first time. The thermal noise in the spectrometer is small; most of the noise apparent in the traces is the quantization noise of the 8-bit digitizer. The signal is equivalent to that of 5×10^{15} polarized protons. The decays shown in Figs. 6(c) and 6(d), were taken 25 min later, when the background signal had begun to recover. The nuclear magnetization was obtained for each free-induction decay by Fourier analysis of signal pairs such as these. A plot of the nuclear magnetization as the background recovers is shown in Fig. 7, trace a. An analysis of such data over 80 h yielded a relaxation time for the background protons of $T_1=30$ h.

The buildup of molecular hydrogen in a freshly prepared cell is shown in Fig. 8. The decays shown in Figs. 8(a) and 8(b) were taken about 10 s after the second saturation and 5 s after the recombination had been initiated. About 10^{16} molecules had been produced in the NMR cavity by this time. Nevertheless, Figs. 8(a) and 8(b) are virtually identical to Figs. 6(a) and 6(b). This observation is consistent with zero nuclear polarization in the newly formed molecules. Alternatively, if the initial polarization can be described by a spin temperature, this temperature is much higher than the ambient temperature of 0.3 K. As the molecules relax to the surface temperature, one expects the NMR signal to gradually increase. This was evident 25 min later as shown in Figs.

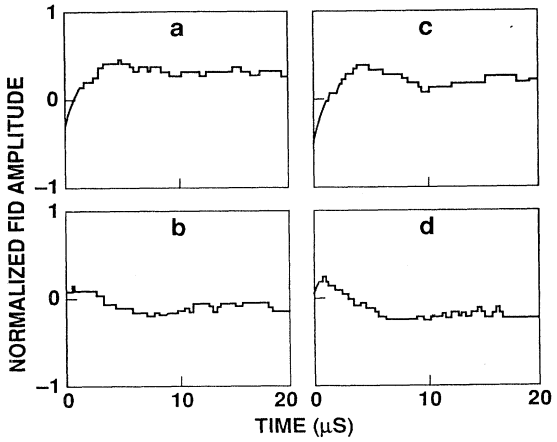

FIG. 6. Free-induction decay signals from background protons in the "empty" cell. One unit of amplitude corresponds to $1.0(3)\times10^{15}$ fully polarized protons. The upper and lower panels are 90° out of phase. Signals *a* and *b* were taken 10 s after saturation; *c* and *d* were taken 25 min later.

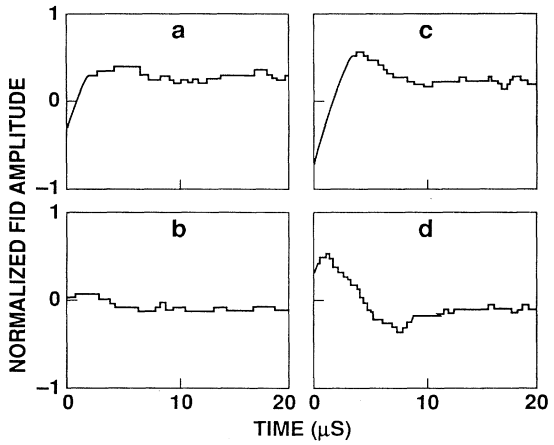

FIG. 7. Free-induction decay signals following the first filling of the cell with molecular hydrogen. Signals *a* and *b* were taken 10 s after saturation of the background and 5 s after the initiation of recombination; *c* and *d* were taken 25 min later. Normalization is identical to that in Fig. 6.

8(c) and 8(d). The signals in Figs. 8(c) and 8(d) are significantly larger than the corresponding background-only signals of Figs. 6(c) and 6(d). The approach of the nuclear magnetization toward thermal equilibrium for the background plus the hydrogen molecules is shown in Fig. 7, curve b.

While the nuclear magnetization in the NMR chamber was relaxing toward thermal equilibrium, the helium-level value was closed to separate the two chambers. Atoms were again loaded into the polarization chamber to prepare for a second filling of molecules. Prior to this second filling, the proton background and the molecular hydrogen already in the NMR chamber were driven into saturation. The decays shown in Figs. 9(a) and 9(b), taken 10 s after this saturation and 5 s into the second filling, are visibly larger than the decays of Figs. 6(a) and 6(b).

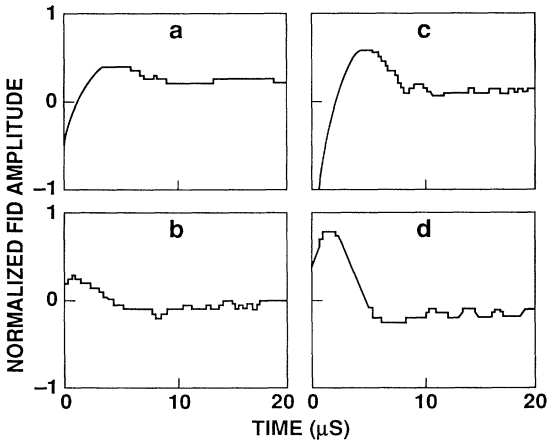

FIG. 8. Free-induction decay signals following the second filling of the cell with molecular hydrogen. Signals *a* and *b* were taken 10 s after saturation of the background and the first fill, and 5 s after the initiation of recombination; *c* and *d* were taken 25 min later. Normalization is identical to that in Fig. 6.

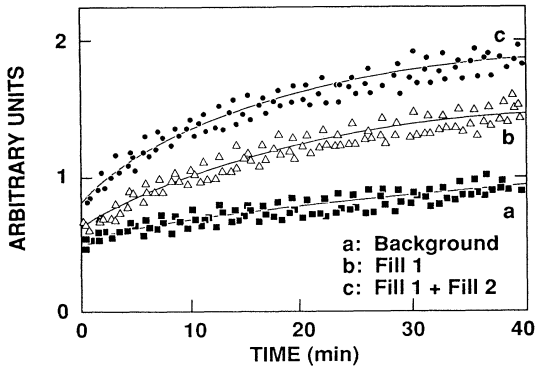

FIG. 9. Evolution of the NMR signal amplitude as the nuclear spins relax toward thermal equilibrium. Trace *a*, background only; trace *b*, background plus first fill; trace *c*, background plus two fills.

This is due to the insufficient saturation of the molecules from the first fill. Subsequently, molecules from both fills relax toward a thermal equilibrium polarization. Signals recorded 25 min later are shown in Figs. 9(c) and 9(d). The evolution of the nuclear magnetization for the background plus the two fills of molecules is shown in Fig. 7 curve c.

In this run, 1.1×10^{17} molecules were added to the cell during each fill. The nuclear magnetization for the molecules alone can be found by subtracting curve a in Fig. 7 from curves b and c. Assuming that the number of ortho molecules remains constant in the 30 min period (molecules are lost due to ortho-para conversion, but the conversion rate is slow), the time evolution of the nuclear magnetization gives the time evolution of the nuclear-spin polarization. The polarization data are shown in Fig. 10 for both the initial fill (a) and the initial plus the second fill (b); the curves are normalized by assuming that the polarization approaches the thermal value of 3.4%.[20] The solid lines in Fig. 10 are fits of the data to the expression,

$$P_n(t)=P_n(0)+[P_T-P_n(0)]\left[1-\exp\left[-\frac{t}{T_1}\right]\right], \qquad (14)$$

which describes the evolution of a nuclear-spin system from an initial polarization $P_n(0)$ to its thermal equilibrium polarization P_T with a relaxation time constant T_1. $P_n(0)$ and T_1 are free parameters in the fitting. The value of $P_n(0)$ depends on the history of the sample. When filling molecules into a pristine cell [Fig. 10(a)], the initial polarization is 0.0(3)%. For the second fill [Fig. 10(b)], the initial polarization is 0.7(3)%. The relaxation-time constant obtained is 11(1) min in both cases.

We interpret the observations as follows. At the time data in Fig. 10 were taken, the molecules were in the solid phase. The near-zero initial polarization for the first fill (when molecules were admitted into a clean cell) indicates that the nuclear polarization had been lost before the solid was several seconds old. The slightly higher initial polarization of the second fill appears to be due to insufficient saturation of the molecules accumulat-

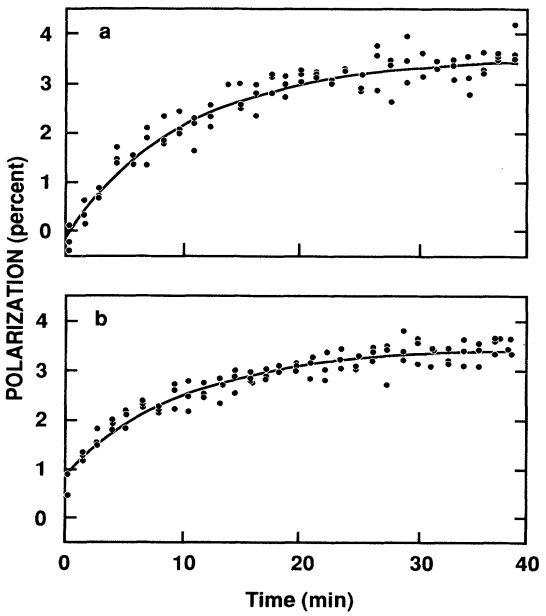

FIG. 10. Relaxation of the nuclear polarization of solid H_2 toward thermal equilibrium at 0.3 K. Trace *a*, background plus first fill; trace *b*, background plus two fills.

ed during the first fill. The long relaxation time precludes the solid being in the hcp phase. The measured relaxation time, $T_1 = 11(1)$ min, agrees well with an empirical formula [Eq. (8)] based on previous NMR measurements on solid hydrogen in the fcc phase.[16] Using $T_1 = 11$ min in Eq. (8) would lead to an ortho concentration of 90%, but we believe that our measurement of the nuclear relaxation time for high concentrations and temperatures are actually more accurate than those upon which Eq. (8) is based.

A separate, more accurate determination of the ortho concentration can be obtained from the ortho-para conversion rate. Once the nuclear magnetization reaches its thermal equilibrium value, the NMR signal amplitude is proportional to the ortho molecule concentration $X(t)$. In Fig. 11, we show the NMR amplitude data over a period of 65 h. The sample was loaded with five consecutive fills, and the total number of molecules was about 5×10^{17}. The sample loading period was about 200 min. The $t=0$ point was set when the sample loading was about half completed. The ortho concentration of solid hydrogen is expected to decay due to ortho-para conversion according to Eq. (9). The concentration is given by

$$\frac{X(t)}{X(0)} = \frac{1}{kX(0)t+1} , \tag{15}$$

where $X(0)$ is the initial ortho concentration and k is the conversion rate constant. Even in the absence of a precise knowledge of the constant of proportionality between the measured signal and the concentration (which would require an accurate value of the filling factor), Eq. (15) allows an accurate determination of the product $kX(0)$. The known conversion rate,[15] $k=0.0190(5)$/h was used together with the measured product to establish that the initial ortho concentration is 99(2)%. A fit of data of Eq. (15) is shown in Fig. 10.

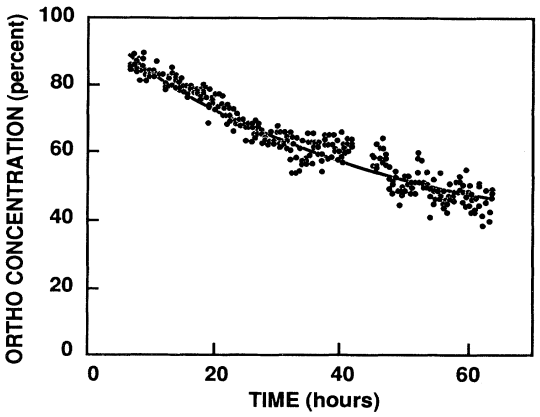

FIG. 11. Ortho concentration during ortho to para conversion in the fcc phase of solid H_2. The solid curve represents Eq. (15) with an initial concentration of 100% and the known conversion rate constant (Ref. 16) $k=0.0190\ \mathrm{h}^{-1}$.

B. Search for initial polarization under other conditions

The observations described above indicate that the atoms recombined into ortho molecules as expected. Contrary to our expectations, however, the nuclear polarization was lost within a few seconds. In an attempt to understand how the polarization was lost, we studied recombination using other procedures, concentrating on the initial nuclear-spin polarization.

The recombination rate was varied by using both higher and lower levels of microwave power to drive the **b**→**c** transition. At the highest power used, 600 μW, recombination is completed within a second. Consequently, the recombination rate is about 10^{17} molecules/s. At this high rate, the heat load on the refrigerator typically drives the cell temperatures above its setting for a few seconds.

Spontaneous recombination following nuclear relaxation of the **a** state atoms was examined when no microwave signal was introduced. The cell temperature was reduced to 0.1 K so that the **b**→**a** relaxation on the surface (followed by **b**+**a**→ortho H_2) proceeded rapidly enough to make accurate polarization measurements possible. Microwave-driven recombination was also carried out at this lower temperature.

Experiments were carried out with a ^{3}He–^{4}He solution as the wall coating. With ^{3}He in the cell, recombination is likely to be dominated by three-body recombination in the bulk because of the reduced probability of adsorption of the hydrogen atoms on the surface and the high-vapor pressure of ^{3}He. At temperatures above 0.5 K, the helium gas density is higher than the density of spin-polarized hydrogen.

None of these procedures produced molecules with an observable initial polarization. To check the unlikely possibility that the polarization was lost by enhanced spontaneous emission, a search was carried out for a

spontaneous radiation signal, but none was detected.

Although we could not detect any initial polarization, the studies with high-recombination rates can be used to set a lower limit for the relaxation rate. If S_N is the sensitivity of the NMR spectrometer in units of polarized protons, and R_N is the recombination rate, then a lower limit to the relaxation rate is

$$T_1^{-1} \approx \frac{R_N}{S_N} . \tag{16}$$

Substituting conservative values of $S_N = 10^{15}$ and $R_N = 10^{16}$ s^{-1}, we have $T_1^{-1} \approx 10$ s^{-1}. Experiments were also carried out with R_N as large as 10^{17} s^{-1}, but in these cases the rise of the liquid-helium temperature complicated the interpretation.

C. Summary of observations

The major features of the experimental observations can be summarized as follows:

(i) On average, each molecule remains in the gas phase no more than 1.5 s. Evidence: the effusion time from the NMR chamber (valve open) is 1.5 s. Even with the valve open, the recombined molecules remained in the NMR chamber.

(ii) The solid phase is fcc. Evidence: the nuclear relaxation time in the solid was found to be 11 min, which is consistent with the fcc phase but incompatible with the hcp phase.

(iii) The molecules formed in the recombination are essentially 100% ortho hydrogen, as expected theoretically. Evidence: the ortho-para conversion rate is consistent with essentially 100% initial ortho conversion.

(iv) The nuclear polarization is lost before the solid is formed. Evidence: if one assumes that the solid is formed at the cell temperature, nuclear relaxation in the solid phase would give an initial polarization consistent with the temperature of the helium film. No such polarization was measured.

(v) The average spin-relaxation rate which destroys the nuclear polarization of the newly formed molecules is greater than 10 s^{-1}. Evidence: a slower rate would have yielded an observable polarization, as described in the discussion of Eq. (16).

VI. DISCUSSION

The disappearance of nuclear polarization in this experiment is puzzling. We based our initial expectations fundamentally on two assumptions: that spin polarization in the gas would be maintained as the molecules cascaded through their excited vibrational and rotational states to the ground state, and that the polarization would continue to be maintained as the molecules aggregated to form an fcc solid.

Although we cannot exclude the possibility of depolarization during the formation of the solid, this seems unlikely. If spin relaxation occurred at this point, the polarization should have had an equilibrium value of 3.4%, consistent with the cell temperature of 0.3 K. The absence of this polarization implies that either the solid was formed at a much higher temperature than the surrounding liquid, which seems implausible, or that it had been lost before aggregation.

Let us turn now to possible sources of depolarization in the gas phase. One can immediately discount "motional" relaxation due to gas phase collisions. In this case it is the fluctuations in the magnetic field at the nucleus caused by the motion of other molecules, or possibly atoms, that causes the nuclear-spin state to change. Low-temperature nuclear relaxation[19] in a spin-polarized hydrogen gas at a density of 10^{16} atoms/cm^{-3} occurs at a rate of $\approx 10^{-4}$ s^{-1}. The dominant interaction in that case is electron-proton. In the gas of ortho H_2, the interaction is proton-proton and is expected to proceed at a rate that is substantially smaller. Such a process cannot account for depolarization on the time scale observed here, approximately 0.1 s.

We next consider the possibility of relaxation due to the interactions within the H_2 molecule itself. Such a molecule in a magnetic field B_0 can be described to good approximation by the Hamiltonian,[21]

$$H = \omega_I (I_{1,z} + I_{2,z}) + \omega_J J_z + \omega' (\mathbf{I}_1 + \mathbf{I}_2)\cdot\mathbf{J} + \omega''[\mathbf{I}_1\cdot\mathbf{I}_2 - 3(\mathbf{I}_1\cdot\mathbf{n})(\mathbf{I}_2\cdot\mathbf{n})] , \tag{17}$$

where $\mathbf{I}_1$ and $\mathbf{I}_2$ are the proton-spin angular momenta, $\mathbf{J}$ is the rotational angular momentum, $\omega_I = \gamma_1 B_0$ is the proton Larmor frequency, $\omega_J = \gamma_J B_0$ is the rotational Larmor frequency, ω' is the coupling strength of the nuclear moments to the rotational magnetic field, ω'' is the coupling strength between the nuclei, and $\mathbf{n}$ is the unit vector connecting the two protons. In a field of 6.7 T, $\omega_J = 2.88\times 10^8$ s^{-1} and $\omega_I = 1.79\times 10^9$ s^{-1}. If the rotation axis reorients so that m_J changes with a correlation time equal to the mean collision time τ_c, then the spin-rotation and dipole-dipole interactions cause longitudinal relaxation at a rate[21]

$$T_1^{-1} = \left[\frac{2J(J+1)}{3}\omega'^2 + \frac{3}{5}\omega''^2 \right] \frac{\tau_c}{1+(\omega_J-\omega_I)^2\tau_c^2} . \tag{18}$$

As will be demonstrated below, the collision time will generally satisfy $(\omega_J - \omega_I)\tau_c \gg 1$, so that Eq. (18) becomes

$$T_1^{-1} = \left[\frac{2J(J+1)}{3} \left(\frac{\omega'}{\omega_J-\omega_I} \right)^2 + \frac{3}{5} \left(\frac{\omega''}{\omega_J-\omega_I} \right)^2 \right] \tau_c^{-1} . \tag{19}$$

To account for the observed relaxation, we must have

$$T_1^{-1} \geq T(\exp)_1^{-1} . \tag{20}$$

$T(\exp)_1^{-1}$ is the experimentally determined upper limit to the relaxation rate, ≈ 10 s^{-1}. We estimate an upper limit to the relaxation rate T_1^{-1} as follows. The coupling constants ω' and ω'' in Eq. (19) are accurately known in the ground state, though not in the excited vibrational and rotational states. On physical grounds, they are expected

to decrease with increasing mean interatomic spacing, and so we can use the ground-state values as an upper limit. These are[22] $\omega' = 7.16 \times 10^5$ s^{-1}, $\omega'' = 1.44 \times 10^5$ s^{-1}. Substituting these values into Eq. (19) shows that the spin-rotational interaction dominates the dipole-dipole interaction, and yields

$$T_1^{-1} \leq 1.5 \times 10^{-7} J(J+1) \tau_c^{-1} . \quad (21)$$

To estimate the collision time τ_c we need to examine the scenario of energy loss from the moment the molecule recombines in the state ($v = 14$, $J = 3$), to its final translational thermalization in the state ($v = 0$, $J = 1$). In the initial stage, when the vibrational number drops from 14 to approximately 6 and roughly 40% of the recombination energy is dissipated, the molecule loses energy extremely rapidly because of the relatively small spacing of the vibrational and rotational states and the high asymmetry of the molecule. Also, in this regime the spin-rotation interaction is expected to be significantly smaller than in the ground state. Consequently, this stage should play a relatively small role in spin relaxation compared to the second stage, when v decreases from six to zero.

Because the probability of energy transfer in an inelastic collision generally increases as the energy gap decreases, the most probable path of deexcitation is a series of rotational transitions to lower values of J followed by a vibrational transition that kicks the molecule up to the nearest rotational level of the next lower vibrational level. The closest rotational transitions in ortho H_2 satisfy $\Delta J = 2$. The maximum value of J following a $\Delta v = -1$ transition in ortho H_2 is $J = 7$. (This rule holds for all of the possible vibrational states.) The energy released in these various steps are as follows. In the sequence of rotational transitions $J = 7 \rightarrow 5 \rightarrow 3 \rightarrow 1$, the energies released are typically 1800, 1300, and 700 K, respectively.[23] In the vibrational transition $(v, J = 1) \rightarrow (v-1, J = 7)$, the energy varies from 1000 K (for $v = 6$) to 1500 K (for $v = 1$). Considering the entire collection of such transitions from the state ($v = 6, J = 7$) to ($v = 0, J = 1$), the mean energy released is

$$\overline{\Delta E} = 1100 \text{ K} . \quad (22)$$

While the molecule is in the liquid, τ_c is so short that the rotational motion is effectively quenched, a point to which we shall return below. Consequently, we focus our attention on the time the molecule spends in the gas. The molecule's kinetic energy will tend to thermalize through gas and surface collisions. From time to time the molecule will undergo an inelastic collision in which energy of about 1100 K is released. To obtain an upper limit on T_1^{-1}, Eq. (19), we shall assume that all of this energy appears as translational energy of the free molecule. From Eq. (21), the mean speed of the molecule is $\bar{v} = 5 \times 10^5$ cm/s^{-1}.

Two processes give rise to collisions with the fast molecules: wall collisions and collisions with the gas in the cell. The mean distance between wall collisions $\overline{l_w}$ is about 1 cm. At the initial densities in the cell, $n \approx 10^{16}$ cm^{-3}, the mean free path for gas collisions $\overline{l_g}$ is approximately 0.1 cm. However, because of the near sphericity of the H_2 molecule, gas collisions are expected to be relatively ineffective in changing M_J. Consequently, the cross section for rotational reorientation is expected to be small compared to the kinetic cross section. In this case, we can take $\tau_c^{-1} = \bar{v}/\overline{l_w} = 5 \times 10^5$ s^{-1}. Substituting this in Eq. (19) yields

$$T_1^{-1} \leq 7.5 \times 10^{-2} J(J+1) \text{s}^{-1} . \quad (23)$$

As an upper limit on J we shall take its likely maximum value, $J = 7$. The result is $T_1^{-1} \leq 4.2$ s^{-1}. We have determined that $T_1^{-1} \leq 0.4 \times T(\exp)_1^{-1}$. It is evident that this result does not satisfy the criterion for relaxation [Eq. (20)]. Since the estimate of the upper limit to T_1^{-1} is believed to be conservative, the disagreement is serious. For instance, it is likely that the average kinetic energy of the molecules is much lower than the average maximum value, 1100 K. According to Eq. (18), this would decrease the relaxation rate. Consequently, for the spin-rotation interaction to be responsible for nuclear relaxation, much of the energy of the molecule would have to be stored in rotational energy, requiring much higher rotational numbers than the energetically favorable limit of $J = 7$. That the molecules would retain rotational energy of over 10^4 K while cooling translationally, seems implausible.

As an upper limit on the possible relaxation rate due to the spin-rotational interaction, we can evaluate Eq. (18) with $|\omega_j - \omega_I| \tau_c = 1$. The result is $T_1^{-1} = 120 J(J+1)$ s^{-1}. This maximum occurs when $\tau_c = 6.6 \times 10^{-10}$ s^{-1}, a condition that could only occur when rotation is essentially quenched within a liquid. However, as described in Sec. II, the vibrational relaxational times for H_2 in liquid H_2 at 14 K is 12 μs. For energy relaxation on such a time scale, it is evident that the spin-rotation interaction is not strong enough to cause nuclear relaxation.

Finally, there is the possibility that the nuclear relaxation is induced by the impurities that gives rise to the background polarization in the cell. This is implausible on several grounds. Because of its resonance characteristics, the background appears to be due to protons rather than a foreign species such as ^{3}He, or some unknown molecule that could give rise to cross relaxation. Since the only substance with a significant vapor pressure at the temperature of the cell is H, the background protons are either on the surface or embedded in it. Even allowing for a tight coupling between the hydrogen molecules and the background impurities, the polarization should not be lost at a rate greater than T_1^{-1} for the background. The most likely interaction, dipole-dipole coupling, is feeble; in any case it would preserve the total nuclear polarization in the cell, which is the quantity measured. The spin-lattice-relaxation rate for the hydrogen molecules interacting with the impurities should be no larger than the spin-lattice rate for the impurities themselves, which is extremely small. In summary, although the background signal is experimentally undesirable, we have not been able to find a mechanism by which it can be linked to the

loss of nuclear polarization of the ortho hydrogen molecules.

The experimental evidence for nuclear relaxation during the recombination of spin-polarized hydrogen appears to be strong. The mechanism, however, remains an enigma.

ACKNOWLEDGMENTS

This work was supported by the Department of Energy through Grant No. DE-AC02-76ET03609, and by the National Science Foundation through Grant No: DMR85-13769.

*Present address: Hansen Labs, Stanford University, Stanford, CA 94305.

†Present address: Department of Physics, Cornell University.

[1]For reviews, see T. J. Greytak and D. Kleppner, in *New Trends in Atomic Physics,* 1982, Les Houches Lectures, edited by G. Grynberg and R. Stora (North-Holland, Amsterdam, 1984), I. F. Silvera and J. T. M. Walraven, in *Progress in Low Temperature Physics,* edited by D. F. Brewer (North-Holland, Amsterdam, 1986).

[2]D. Kleppner and T. J. Greytak, in *High Energy Spin Physics (Brookhaven National Laboratory and Westhampton Beach, New York),* Proceedings of the Fifth High Energy Spin Symposium, AIP Conf. Proc. No. 95, edited by G. M. Brunce (AIP, New York, 1982).

[3]R. M. Kulsrud, H. P. Furth, E. J. Valeo, and M. Goldhaber, Phys. Rev. Lett. **49**, 1248 (1982).

[4]R. M. More, Phys. Rev. Lett. **51**, 396 (1983).

[5]The fact that the ortho concentration produced in these recombinations is very high and not at the thermal equilibrium value has been described briefly: Y. M. Xiao, S. Buchman, L. Pollack, D. Kleppner, and T. J. Greytak, J. Chem. Phys. **96**, 4032 (1992).

[6]J. M. Greben, A. W. Thomas, and A. J. Berlinsky, Can. J. Phys. **59**, 945 (1981).

[7]Y. Kagan, I. A. Vartanyants, and G. V. Shlyapnikov, Zh. Eksp. Teor. Fiz. **81**, 1113 (1981) [Sov. Phys. JETP **54**, 590 (1981).

[8]C. Schwartz and R. J. LeRoy, J. Chem. Phys. **81**, 4149 (1984).

[9]M. M. Audibert, C. Joffrin, and J. Ducuing, Chem. Phys. Lett. **25**, 158 (1974).

[10]M. H. Alexander, Chem. Phys. Lett. **38**, 417 (1976).

[11]C. Delande and G. M. Gale, Chem. Phys. Lett. **50**, 339 (1977).

[12]R. I. Hall, I. Cadez, M. Lamdau, F. Pichou, and C. Schermann, Phys. Rev. Lett. **60**, 337 (1988).

[13]P. J. Eenshuistra, J. H. M. Bonnie, J. Los, and H. J. Hopman, Phys. Rev. Lett. **60**, 341 (1988).

[14]K. E. Kurten and M. L. Ristig, Phys. Rev. B **31**, 1346 (1985).

[15]I. F. Silvera, Rev. Mod. Phys. **52**, 393 (1980).

[16]N. S. Sullivan and R. V. Pound, Phys. Rev. A **6**, 1102 (1972). Note, the expression for the parameter B in our text is the one determined by Sullivan and Pound for concentrations $x > 0.56$.

[17]F. Weinhaus and H. Meyer, Phys. Rev. B **7**, 2974 (1973).

[18]I. F. Silvera, Phys. Rev. B **29**, 3899 (1984).

[19]D. A. Bell, H. F. Hess, G. P. Kochanski, S. Buchman, L. Pollack, Y. M. Xiao, D. Kleppner, and T. J. Greytak, Phys. Rev. B **34**, 7670 (1986).

[20]In principle, one can use Eq. (11) to calculate the nuclear magnetization without assuming that it approaches a thermal value. But the filling factor for the small amount of solid produced here will not be the same as for the calibration gas. Instead, we assume that the nuclear spin relaxes to the thermal value of 3.4% and derive the filling factor for the solid sample from Eq. (11). The derived filling factor, 0.22(5), is about a factor of 2 larger than the filling factor of the gas sample. This is to be expected because the solid is distributed at the surface of the NMR cavity where the rf magnetic field is larger than the average.

[21]N. F. Ramsey, *Molecular Beams* (Oxford University Press, London, 1956).

[22]A. Abragam, *Principles of Nuclear Magnetic Resonance* (Oxford University Press, London, 1983).

[23]W. Kolos and L. Wolniewicz, J. Chem. Phys. **49**, 404 (1963).